Algerian Journal of Environmental Science and Technology
March edition. Vol.8. Nº1. (2022)
ISSN : 2437-1114
www.aljest.org

Surface Modification of Olive Stone-based Activated Carbon for Nickel Ion removal from synthetic wastewater

M.Termoul [1], B. Bestani[1], N. Benderdouche[1], M.A. Chemrak[1,2,*], S. Attouti[1]

[1] Laboratory of Structrure, Elaboration and Applications of Molecular Materials (SEAMM), University Abdelhamid Ibn Badis of Mostaganem (UMAB), Faculty of Science and Technology, B.P.227, Mostaganem 27000, Algeria.
[2]Institute of Science and Technology, University Center of Tissemsilt, Road of BOUGARA, Ben Hamouda, Tissemsilt 38004, Algeria.

* Corresponding author: mohammedamin.chemrak@univ-mosta.dz; Tel: + 213 675 94 61 64.

ARTICLE INFO

Article History :
Received ***:20/04/2020***
Accepted ***:01/10/2020***

***Key Words*:**

Olive stone-based Activated Carbon ;
Surface Modification ;
Surface Properties;
Nickel Removal.

ABSTRACT/RESUME

Abstract: *The aim of this work is to investigate nickel ion removal from its aqueous solutions by an olive stone-based activated carbon. Activated carbon surface properties modification was carried out nitric acid (4 N) as an agent for Ni(II) adsorption capacity improvement. The originally prepared and modified activated carbons were characterized by FT-IR spectrometry, X-ray diffractometry, Scanning electron microscopy (SEM), X-ray photoelectron spectrometer (XPS), N_2/77 K BET analysis, pH_{PZC} and iodine number determination. Nickel ion adsorption capacity was enhanced by 3.6 times while the specific surface area increased by 24% due to chemical treatment. The effect of relevant parameters on Ni(II) uptake such as contact time, adsorbent dose, pH, kinetics was also examined. An activated carbon dose of 4 $g.L^{-1}$and a contact time of 120 min and respective corresponding values of 8 g/L and 180 min for the treated and untreated activated carbons were required to reach equilibrium for a 100 $mg.L^{-1}$initial solution concentration. The highest adsorption performance was achieved by the acid-modified activated carbon samples in the pH range of 5.5-6.5. Experimental data was correlated by non-linear Langmuir and Freundlich adsorption models. Langmuir isotherm provides a slightly better fit to the experimental data indicating homogeneous distribution of adsorbents active sites with monolayer adsorption. Three methods of error analysis of residual root mean square error (RMSE), chi-square error (χ^2) and average percentage error (APE) were used for best fit-isotherm and kinetic models identification. Langmuir is more representative with high (R^2) low RMSE and good χ^2. Second-order kinetics and intraparticular diffusion were found to describe Nickel adsorption of both investigated materials.*

I. Introduction

In the last decades, increasing population and industrialization have led to increasing environmental problems destroying then the ecologic system and exhausting rapidly clean resources. Environmental pollutants such as heavy metals are major pollutants occurringin marine, soil and wastewater can be a real threat for many life forms due to their toxicity [1, 2]. Among them, Nickel ion (Ni(II)) is classified as a toxic heavy metal that could pollute the water environment and beharmfull to human body [3] by causing a disorder known as nickel-eczema. Large consumption of food and beverages rich in nickel can lead to serious disease.

A variety of methods can be used for the removal of heavy metals from wastewater including chemical precipitation [4], solvent extraction [5], ultrafiltration [6], biochemical treatment [7], ion exchange [8] and adsorption [9–13]. The latter, considered as a third stage of wastewater treatment, has been preferred over the above-mentioned processes because of its cheapness and high-quality effluent treatment. Adsorption is the process by which a solid adsorbent can attract a component from the aqueous phase to its surface, thereby forming an attachment via a physical or chemical bond, thus removing the component from the aqueous phase. Among a large variety of solids available in the market, activated carbon is the most effective adsorbent used to date. However, other different cheaper adsorbents have been used; some of them are still under investigation for heavy metal elimination such as peat [14] and marine algae [15]. Different low-cost materials including clays, maize cob, bagasse and palm fruit bunch have also been used to remove heavy metals from water [16]. In addition, microorganisms have also been found to be effective in removing heavy metal ions [17, 18]. Many studies have reported the use of adsorption by activated carbon for the removal of Ni(II) from aqueous solutions [19, 20]. Activated carbon commercially available or locally prepared can be modified by several chemical or physical treatments to incorporate or eliminate functional groups changing then its surface chemistry [21].

Nitric acid is known as a very strong oxidizing agent for carbonaceous materials, it is mainly used to generate carboxylic and lactons functions [22]. This kind of treatmentcan also createcarboxylate functions [23]. A recent study [24] has shown that the oxidation of an activated carbon made from petroleum coke by this acid is much more drastic than with H_2O_2: this can be explained by its stronger oxidizing strength allowing it to introduce more functional groups and developing the porous structure.

The objective of the present work is to study some parameters influencing the adsorption of Ni(II) by an activated carbon prepared locally from olive stones chemically activated by nitric acid [25] for adsorptive capacity enhancement toward the considered metal ion and to compare the physicochemical properties obtained to the Merck commercial activated carbon, in order to explain the mechanism for Ni(II) adsorption. Prior to adsorption tests, parameters influencing Ni(II) uptake such as contact time, adsorbent doses, pH and temperature were also conducted. In this study, binding characteristics of Ni(II) on four prepared samples and feasible application of two adsorption models were investigated. The isotherm constants for the Langmuir, Freundlich isotherms and kinetic parameters have been calculated using non-linear regression with the help of OriginPro (Version8.5) software program.

II. Materials and methods

II.1. Surface Modification

Two types of activated carbons withchemically modified surfaces were used in this study for nickel ions removal from synthetic solutions. Amass of 20 g of a locally prepared activated carbon from olive stone and a commercially available one from Merckwere treated separately with 100 mL of HNO_3 (4 N) under reflux for different time intervals of 2, 4 and 6 hours at 80 °C. After separation, the solid phase was then rinsed with sodium hydroxide in order to neutralize excess acid then with hot water until neutral pH. The prepared samples were oven dried at 60°C overnight then grinded and sieved to obtain powdered particles with a diameter $\leq$ 0.071 mm. Four different types of activated carbons were prepared, which are referred to as OS-AC (olive stone-based activated carbon), MOS-AC (modified activated carbon from olive stones), C-AC (commercial activated carbon) and MC-AC (modified commercial activated carbon).

II.2. Characterization of activated carbons

The prepared samples were characterized using B.E.T test for surface area determination; a manometric N_2 adsorption Sorptomatic apparatus was used for this purpose in which samples of 0.04 g were degassed at 573 K for 4 h [25]. Iodine number, defined as the number of milligrams of iodine adsorbed per gram of activated carbon at a residual concentration of 0.02 N was determined for sample microporosity indication according to ASTM D4607 standard [26]. Scanning electron microscopy (SEM) method was also performed for observation and comparison of the external surface of the samples before and after modification. By (deposition of metal layers) in a sprayer Powder X-ray diffraction (XRD) patterns were recorded with Cu Kα1 (λ=1.54059 Å) radiation in the 2θ range of 10–90° on a diffractometer (Rigaku D/Max2200) in which a two-stepsample preparation was carried out, drying (heating to 80°C) the materials followed by metalization.

XPS measurements were performed on a Kratos Axis Ultra using AlKα (1486.6eV) radiation apparatus. High resolution spectra were acquired at 20 eV pass energy with energy resolution of 0.9 eV. The C1s line of 284.5 eV was used as a reference to correct the binding energies for charge energy shift.

In addition, the surface functional groups of the samples were determined by means of Fourier transform infrared spectrometer (FT-IR). IR analysis is carried out on KBr tablets manufactured in the following proportions: Each sample was mixed with potassium bromide in 0.1 wt. % Ratio and used for FT-IR analysis. Samples were dried under vacuum at 110 °C prior to mixing with KBr powder. The mixture was finally grinded and then

vacuum dried at approximately 110 °C [27]. The solid phase IR absorption spectra were recorded in the range of 4000 and 400 cm^{-1} with the infrared spectrometer type (SHIMADZU-IR Prestige-21) for all prepared samples before and after the modification. Finally, another important parameter for all samples was determined, the point zero charge (pHpzc). It indicates the net surface charge of an adsorbent in solution [28, 29]. In this case, 50 mL of NaCl solution (0.01 M) were placed in different cap vials, their initial pH was adjusted from 2 to 11 by adding sodium hydroxide or concentrated hydrochloric acid. Once a constant value of initial pH is reached and noted (pHi), 0.15 g of prepared activated carbonsis then added to the NaCl solutions. The mixture is agitated for 48 hours and the final pH values were measured and noted (pHf). A plot of pHf versus pHi from which the pHpzc value is obtained, value at which pHf = pHi [30].

II.3. Nickel adsorption experiments

Nickel ion stock solution was prepared by dissolving 1 g of $NiCl_2.5H_2O$ in 1L of deionized water. Successive dilutions were used to obtain working solutions of desired concentrations. Analytical reagent-grade chemicals were used for solutions preparation.

Prior to Ni(II) adsorption experiments in batch mode at ambient temperature, parameters affecting the removal rate such as initial concentration ranging from 10-900 $mg.L^{-1}$, contact time ranging from 30-480 min, adsorbent dosage raging from 2-24 $g.L^{-1}$ and pH ranging from 2-7 were performed before and after surface modifications of each adsorbent.

A 0.1 g of each activated carbon was added separately in 25 mL of nickel solutions with known initial concentrations, and the mixture was agitated magnetically until equilibrium and then centrifuged at 4000 rpm and the Ni(II) residual concentrations determined using a UV-visible 9582 Optizen spectrophotometer at 465 nm using dimethyglyoxime (2.5%) as complexing agent [31]. Reported studies showed that dimethylyoxime has a high affinity in detecting Ni(II) traces [32]. The adsorbed amount of Ni(II) at equilibrium is calculated using equation (1) [33] :

$$q_e = \frac{(C_0 - C_e)\cdot V}{m} \quad (1)$$

Where : V is the volume of the liquid phase (mL), C_o and C_e are the initial and the equilibrium concentrations of Ni(II) ($mg.L^{-1}$), and m the mass of the activated carbon sample (mg).

II.4. Error analysis

Non-linear regression analysis using OriginPro8.5 was evaluated in the present study for adsorption and kinetic parameters evaluation. Several error analysis methods such as the correlation coefficient (R^2), Chi-square analysis (χ^2), root mean square error (*RMSE*) and the Average percentage error (*APE*) given by equations (2, 3 and 4)were used in order to confirm the best-fitting models [34]. In general, smaller values of χ^2 indicate similarity between the data obtained using a model and the experimentally one (larger χ^2 values will increase the difference between the model and experimental data) and the better the curve fitting occurs with small *RMSE* value. Models converge and become favorable with lower values of error functions.

Chi-square statistic: $\chi^2 = \sum \frac{(q_{e,exp} - q_{e,cal})^2}{q_{e,cal}}$ (2)

Roots mean square error:

$$RMSE = \sqrt{\left(\frac{1}{N-2}\right)\cdot \sum_1^N \left(q_{e,exp} - q_{e,cal}\right)^2} \quad (3)$$

Average percentage error:

$$APE = \left(\sum_1^N \left(\left|q_{e,exp} - q_{e,cal}\right|/q_{e,exp}\right)/N\right)\cdot 100 \quad (4)$$

Where, $q_{e,exp}$, $q_{e,cal}$ ($mg.g^{-1}$) represents the experimental and calculated adsorption capacity values, respectively, and N is the number of observations in the experimental data.

III. Results and discussion

III.1. Physical and chemical properties of the activated carbons

The B.E.T method is used in this study to evaluate the adsorption data and generate a specific surface area result expressed in ($m^2.g^{-1}$) of our samples. These values measured on the prepared activated carbons using N_2 adsorption isotherm at 77K are listed in Table 1. They were evaluated from the linearized B.E.T isotherm $\frac{1}{V\left[\left(\frac{P_0}{P}\right)-1\right]}$ vs $\left(\frac{P_0}{P}\right)$ plots in the application range of $0.055 < \frac{P_0}{P} < 0.30$.Were $\frac{P_0}{P}$ represent relative pressure and V is the volume of N_2 adsorbed at standard temperature and pressure.

As we can see from Table 1, the specific surface area of the modified sample by nitric acid increases slightly by 27 $m^2.g^{-1}$ while its microporosity remains almost constant as indicated by the iodine number.

Nonetheless, a decrease of 188 $m^2.g^{-1}$ in B.E.T surface area of MC-AC is noticed. This decrease is may be due to the activated carbon walls collapse and the surface area decrease by pore volume reduction as reported in adsorption textbooks.

The considerable changes in the activated carbon surface area could be associated with two possible effects: i) the partial destruction of the micropores walls and ii) decrease in the total specific surface area and volume of the micropores, which is explained by the presence of oxygenated groups at

the entrance of the pore walls [35]. Another reason for this decrease in the B.E.T specific surface area can stem from a blockage of micropores caused by the formation of humic substances or surface oxides during the oxidation process [36]. Nitric acid partially disrupts pore texture, as observed in the study of the decrease in the B.E.T specific surface area of C-AC. Iodine number is a fundamental parameter to characterize the performance of activated carbons. It is a measure of the micropore (0–20 Å) content of the activated carbon by simple adsorption of iodine in aqueous solution. The typical range is 500-1200 $mg.g^{-1}$ equivalent to

Table 1. Physical parameters of all adsorbents before and after modification

Adsorbent	OS-AC	C-AC	MOS-AC	MC-AC
BET Surface area ($m^2.g^{-1}$)	1257	1031	1284	843
Iodine number ($mg.g^{-1}$)	1012	828	1016	496

Abbreviations : *OS-AC, olive stone-based activated carbon; C-AC, commercial activated carbon; MOS-AC, modified activated carbon from olive stones; MC-AC, modified commercial activated carbon.*

a surface area of activated carbon between 900 and 1100 $m^2.g^{-1}$ [37]. From Table 1, we can say that the two activated carbons with better porosities of 1016 $mg.g^{-1}$ and 1012 $mg.g^{-1}$ are MOS-AC and OS-AC respectively comparing favorably with other materials [38]. The micropore content on the surface of activated carbon increases slightly during modification. The oxidation with nitric acid leading to increased release of CO_2 and CO gas and creating micropores inside mesopores. The iodine number for MC-AC is 496.52 $mg.g^{-1}$ compared to C-AC which is 828.14 $mg.g^{-1}$, this can be explained by the fact that the pore volume has decreased due to the increase in functional groups on the surface of the modified activated carbon, causing the pores from clogging.

III.2. XRD patterns

The XRD patterns of all adsorbents are shown in Fig.1. They display similar XRD profiles and exhibit broad diffraction peaks at 2θ=24.2° and 43.6 °, corresponding to the 002 and 100 diffraction planes of graphite [39, 40]. The 002 plane presents a narrow peak with steep rise, and the 100 plane displays a broad small diffraction peak. The amorphous nature of the samples is confirmed by the obtained X-ray powder diffraction patterns which shows a single large peak centered at about 2θ = 24° in accordance with the literature [41]. That means that the nitric acid modification process has little influence on the amorphous nature of the activated carbons studied.

III.3. Scanning Electron Microscopy (SEM) Analysis

Samples were characterized with Field Emission Gun Scanning Electron Microscopy (FEG-SEM) performed on a JEOL JSM 7600 F apparatus. Images were obtained at an acceleration voltage of 15 kV.

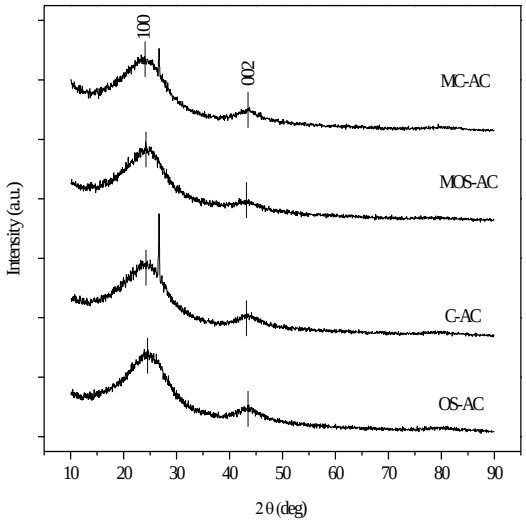

Fig 1. *XRD diffraction patterns of OS-AC, C-AC, MOS-AC and MC-AC*

Figs. 2 and 3 show the surface images of the activated carbons before and after modification. The same characterization technique was used to analyze the unmodified, modified material and after adsorption [42]. Figs. 2 and 3 show the surface images of the activated carbons before and after modification. In Figs. 3a and 3b, the images representing OS-AC and MOS-AC, did not reveal significant morphological differences. In contrast the SEM analysis of commercial activated carbon before and after modification clearly shows that the latter has irregular cavities and a well-developed porous structure. The higher the number of pores, the more accessible the adsorption sites are, which increases the amount of Ni(II) removed. For MC-AC (Fig.3b) the analysis was performed at ×3000 magnification. The image shows that the pores of the commercial activated carbon disappear after oxidation with nitric acid. The results can be

supported by the results of the B.E.T analysis (Table 1).

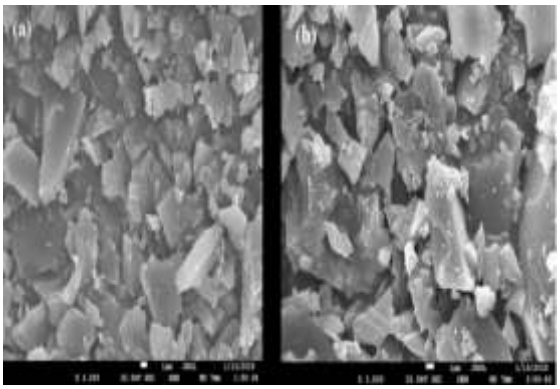

Fig 2. *SEM micrographs of olive stone-based activated carbon, (a) OS-AC, magnification 3000x ; (b) MOS-AC, magnification 3500x*

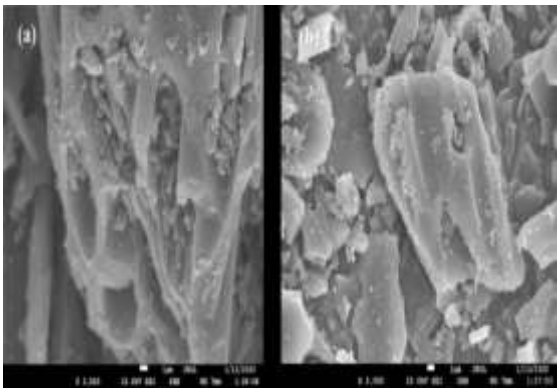

Fig 3. *SEM micrographs of commercial activatedcarbon, (a) C-AC, magnification 3500x; (b) MC-AC, magnification 3000x*

III.4. XPS results

The samples were analyzed by XPS are shown in Figs. 4 and 5. For all activated carbons studied, the survey spectra show intense peaks at 532.0 eV and 284.0 eV indicating the presence of oxygen and carbon, respectively [43]. The survey spectra also show a weak nitrogen peak. For OS-AC the C 1s peaks can be adjusted in five independent sub-bands which are assigned to carbon in the binding states C-C (284.4 eV), C-H (285.8 eV), C-OH (286.6 eV), C-O (287.7 eV) and C=O (carbonyl groups) at 288.7 eV. In addition, the O 1s peaks were deconvoluted into three peaks at 531.7 eV due to the presence of OH and C-O groups, at 532.7 eV could be due to the presence of C-OH bonds and one peak at 533 eV was attributed to C-O-O groups. The presence of C-O, C=O and OC=O groups on activated carbons surface and many others are to be expected given the oxidation state of the raw material whether thermally (steam carbonization) and chemically (H_3PO_4, HNO_3) [44]. The weak N 1s spectrum was deconvoluted into a single peak at 405.7 eV due to the presence of the O-N-O bonds. After oxidation with nitric acid, the intensity was reduced because oxygen groups were formed on the surface of the modified activated carbon. For MOS-AC, the C 1s peaks are very similar to those of OS-AC. The deconvolution of the signal attributed to oxygen (O 1s) identified four peaks corresponding to oxygen atoms involved with carbon and hydrogen bonding at 531.4 eV and 532.8 eV, which are attributed to OH groups (alcohols or phenols), CO and C-O-C, respectively, chemisorbed oxygen at 530.4 eV [45]. Regardless of the oxidized activated carbons, their graphitic carbon content (at 284.0 eV) is lower than that of raw carbon. It is also noted that the percentages of oxygen bonded to carbon increased after oxidation [46].

XPS analysis of the commercial activated carbon confirmed, after deconvolution of the C 1s spectrum, a slight oxidation of MC-AC compared to C-AC. For C-AC the deconvolution of the signal attributed to the carbon (C 1s) allowed the identification of seven peaks corresponding to carbon atoms involved with oxygen and metal ion bonds (283.6 eV). The deconvolution of the O 1s signal indicates that the intensity of the O=C bonds is higher than that obtained by the deconvolution of the C 1s signal. Chemisorption of oxygen and the O=C-OH groups were detected at 531.0 eV, the O=C-OH groups can be attributed to carboxylic groups, esters or lactones.

For MC-AC, the C 1s spectrum includes four peaks with deconvolutionally differentiated binding energy values corresponding to C-C and C-H (graphitic carbon) at 284.7 eV and 285.6 eV, respectively. The deconvolution of the C 1s spectrum is characterized by two further peaks one is assigned to the C-OH (alcohol) groups at 286.4 eV and the other is assigned to the C=O (carbonyl) groups at 288.6 eV. For oxygen, the three adjusted components corresponded to C-O groups (ketone, lactone, ester and carboxyl) and OH (hydroxyl) groups at 531.7 eV and C-O-C (ether-oxide) groups at 532.9 eV. Nitrogen functionalities at the surface of MC-AC are characterized by a single peak, which has been assigned to the O-N-O groups at 405.7 eV [47]. XPS analysis confirms the high oxygen content on the surface of C-AC.

III.5. FT-IR analysis

The FT-IR spectra of the samples used in this study areshown in Fig.6. Analyses of these spectra show the presence of a range of functional groupments on activated carbons the surfaces.

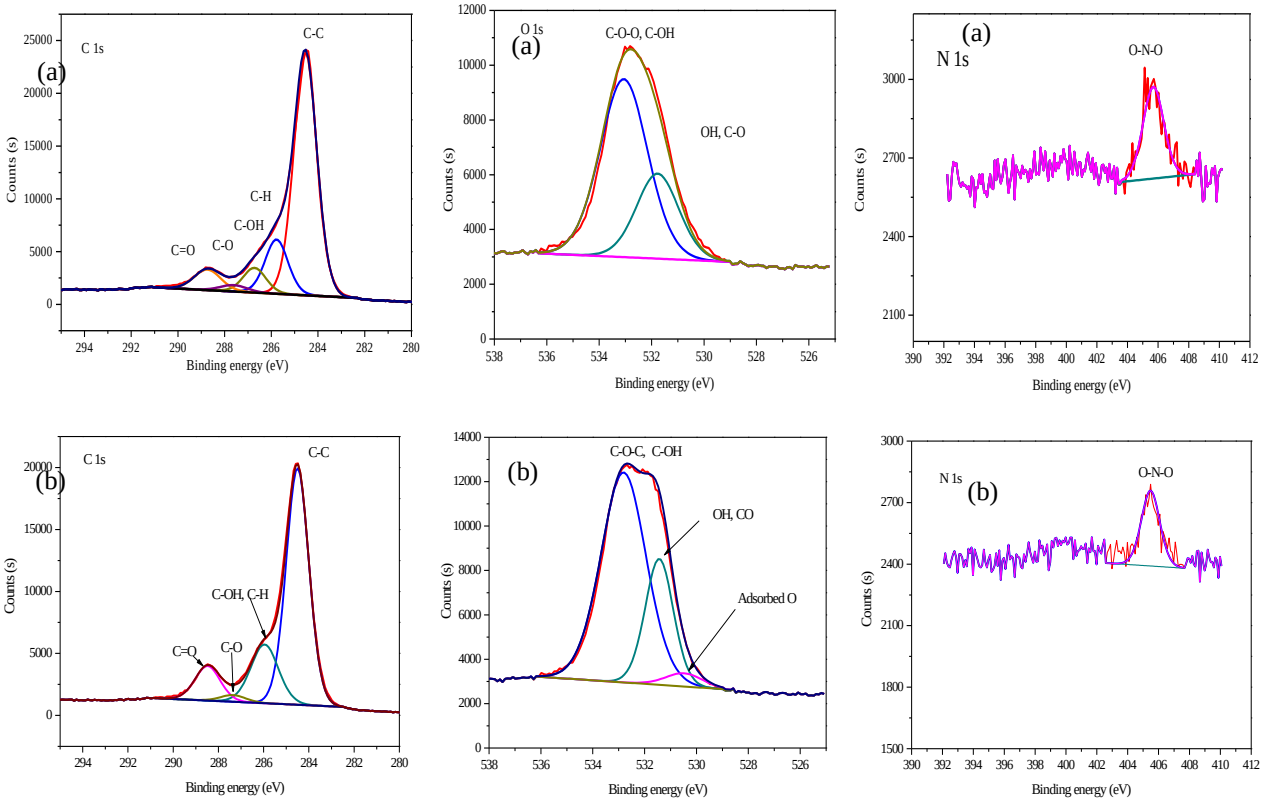

Fig 4. *XPS spectra of olive stone-based activated carbons, (a) OS-AC, (b) MOS-AC*

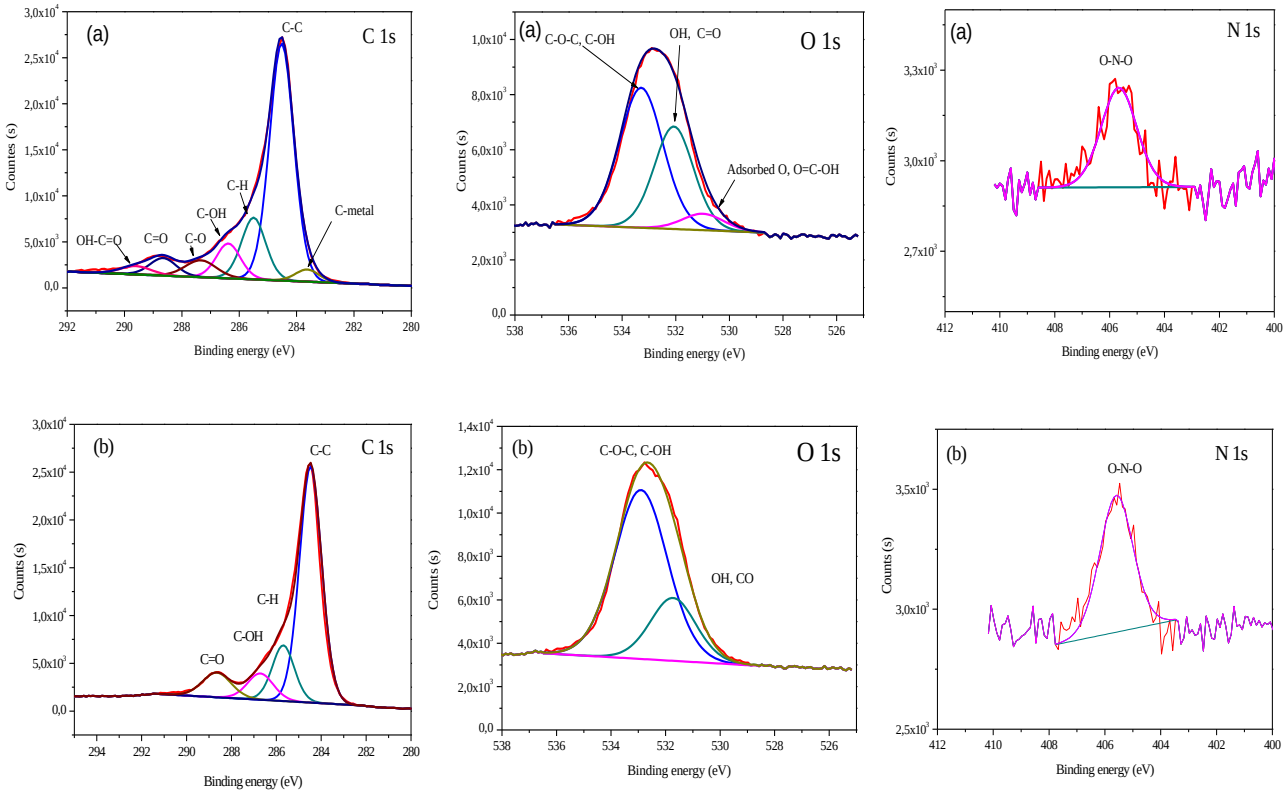

Fig 5. *XPS spectra of commercial activated carbons, (a) C-AC, (b) MC-AC*

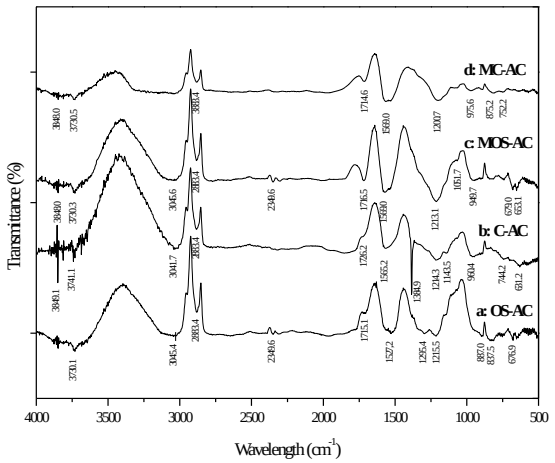

Fig 6. *FT-IR spectra of all samples, a) OS-AC, b) C-AC, c) MOS-AC and d) MC-AC*

In most cases, the studied adsorbents have similar absorption bands, with only difference in their transmittance, indicating small differences in the surface chemistry. The changes in the absorption bands are mainly caused by the oxygen-containing acidic surface groups introduced by oxidation with HNO_3. For all activated carbons a weak absorption band of about 3800-3300 cm^{-1} corresponds to an associated peak of hydroxyl groups of phenols, alcohols and absorbed water [22, 48]. The broad absorption hydroxyl band for OS-AC and MOS-AC can be attributed to the presence of a larger number of -OH groups, possibly due to phenolic groups after the activation process and oxidation with nitric acid. Spectra bands around 2349 cm^{-1} for OS-AC and MOS-AC are due to ketene or ketone [49]. For all activated carbons, a distinctive broad absorption band is in the range of 1705 to 1726 cm^{-1}, attributed to C=O stretching vibrations of saturated carboxylic acids and lactone groups. A peak at 1565 cm^{-1}, corresponding to the N-H group, was found for C-AC, MC-AC and MOS-AC [50]. For OS-AC, a broad absorption band in 1527.2 cm^{-1} indicates the presence of a stretching vibration of NO_2 can also be attributed to N=N vibrations. In the region 1300–1400cm^{-1}, a strong absorption band at 1384.9 cm^{-1} for C-AC corresponds to stretching vibrations of C–N bonds [51]. The new weak peak appeared in MOS-AC at 1066.7 cm^{-1} after the modification with nitric acid indicates the presence of the C-N vibration [52]. Two new absorption peaks appeared for MOS-AC at 1057.7cm^{-1} which corresponds to the stretching vibration of C-N in the amine group [53] and 875.2 cm^{-1} for MC-AC associated with the stretching vibration of the N-H bond in the amine group [54]. On the whole, the same carboxylic functions, alcohol, phenol and lactons are found in the activated carbons. The FT-IR spectra of modified activated carbons with nitric acid did not reveal any significant changes in the groups present on the surface of the adsorbents. The results of FT-IR were consistent with the results obtained by XPS. These results showed that modification with nitric acid could indeed increase the functional groups containing O and N on the studied activated carbons.

III.6. pHpzc

pHpzc values are shown in Figs.7 and 8. The modification of the olive stone-based activated carbon by nitric acid increases the acidic functional groups (carboxylic, lactonic and phenolic), this decrease has totally changed the pHpzc of OS-AC from 6.22 to 3.63. *Shuheng Yao et al.* have shown that the pHpzc of activated carbon obtained from rice husk modified by nitric acid under microwave heating decreased from 6.0 to 4.6, due to the increase in acidic functional groups on the surface of the activated carbon [55]. The oxidation of the C-AC does not have much influence on the surface charge; a slight decreasefrom the pHpzc 6.44 to 6.07 has been noticed. This result can be attributed to the cation exchange that occurs between H^+ surface acid groups and Ni(II) in solution. This is manifested by a decrease in the pH of the treated solution. At pH<pHpzc, repulsion occurs as long as both the surface of the activated carbon and Ni(II) are positively charged implying a decrease in adsorption capacity. On the other hand, at pH>pHpzc, there is an attraction between positively charged Ni(II) and the negatively charged surface of activated carbons, implying an increase in adsorption capacity. These results indicate that the surface chemistry of the studied adsorbents is not sufficient to explain the adsorption phenomenon. A physical characterization to determine the specific surface area and porosity of the samples seems necessary to us to explain the adsorption of Ni(II) on these materials.

III.7. Effect of contact time

The study of adsorption of a compound on an adsorbent allows us to examine the influence of contact time on its retention. This study was conducted to determine the fixed amount of nickel in the range of 30– 480 min of agitation. In order to determine the adsorption equilibrium times, a volume of 25 mL of solution of nickel with initial concentration of 100 $mg.L^{-1}$ at initial pH arbitrarily chosen. The solution was contacted with 0.1 g of each sample separately. Solutions were analyzed for equilibrium concentration (Ce) determination after times ranging from 30 to 480 min.

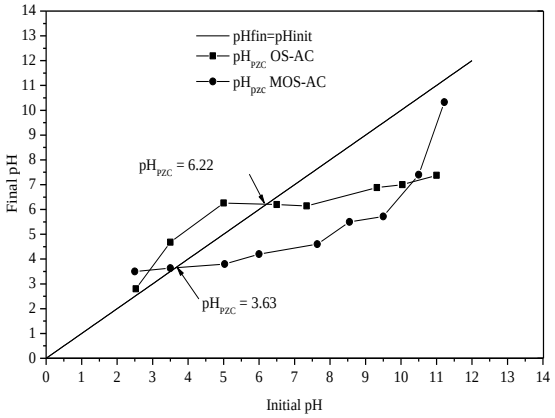

Fig 7. *pH_{pzc} of OS-AC and MOS-AC*

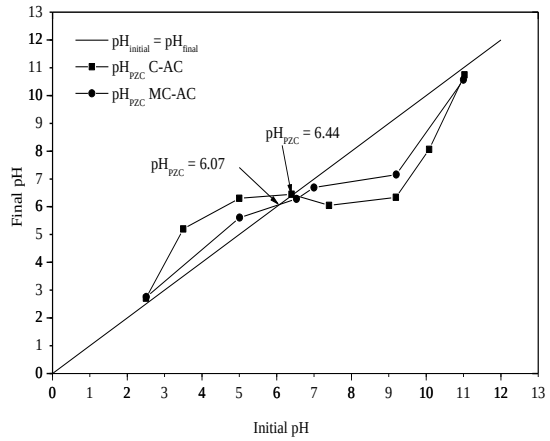

Fig 8. *pH_{pzc} of C-AC and MC-AC*

Fig.9 shows the effect of contact time on adsorption of Ni(II) onto four activated carbons. It clearly indicates that there is a rapid increase in timeand uptake of Ni(II) in the initial stages, but became stable in the finalones till equilibrium is attained. The same figure shows that the equilibrium is reached quite quickly about 120 min for Ni(II) with modified activated carbons (MOS-AC) compared to 180 min for unmodified carbons (OS-AC) and 360 min for C-AC. Kinetic adsorption of Ni(II) was rapid in the first 90 min because the adsorption sites were vacant, and Ni(II) could easily interact with these sites. These results also indicate that the surface modified activated carbon can remove Ni(II) more effectively from the solution compared with untreated activated carbon.

The high adsorption capacity of Ni(II) confirms that the adsorption process is not only related to the specific surface area, pore specific volume and mean pore diameter of the absorbent, but also dependent on the content of surface oxygen-contained functional groups [56]. These equilibrium times used are assumed to be amply sufficient for all experiments.

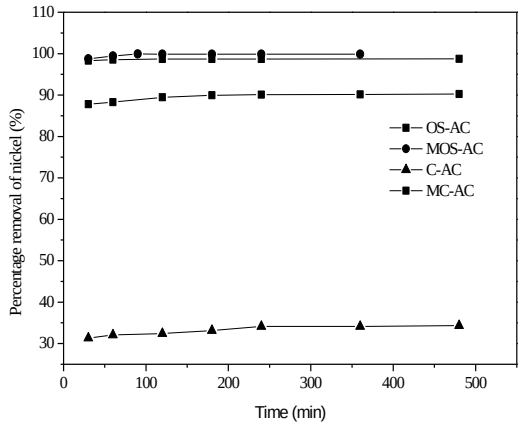

Fig 9. *Effect of contact time on the percentage removal of Ni(II) onto the OS-AC, C-AC, MOS-AC and MC-AC (C_0= 100 mg.L^{-1})*

III.8. Effect of adsorbent dose

Adsorbent dose effect is a very important parameter to find out the optimum amount of activated carbon required for the removal of Ni(II) metal ions. This was done with different doses of activated carbons ranging from 4 to 24 g.L^{-1} for the initial concentration of 100 mg.L^{-1} at equilibrium times previously determined for each adsorbent and pH (5-6). The dose effects on the removal of Ni(II) ion are shown in Fig.10. The percentage removal of Ni(II) increased as the adsorbent dose increased which may due to increased adsorbent surface area and availability of more adsorption sites [57]. It was noted that the optimum adsorbent dosesof 4 g.L^{-1} (MOS-AC), 8 g.L^{-1} (OS-AC), 16 g.L^{-1} (MC-AC) and 16 g.L^{-1} for C-AC were chosen for further experiments. *A. Edwin Vasu* reported that the optimal dose for removal of Ni(II) onto modified activated carbon from coconut shells with nitric acid is 2 g.L^{-1} [58].

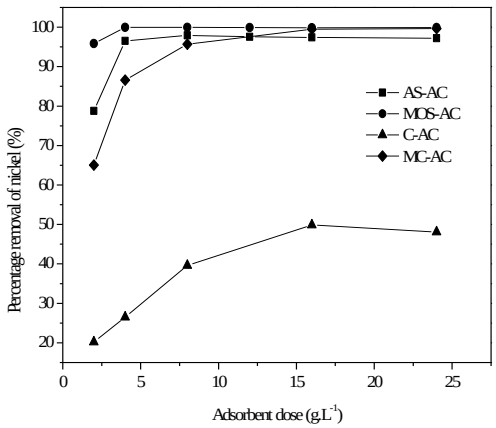

Fig 10. *Effect of adsorbent dose on the percentage removal of Ni(II) onto the OS-AC, C-AC, MOS-AC and MC-AC,(C_0= 100 mg.L^{-1})*

III.9. Effect of pH value

Solution pH is one of the major factors affecting adsorption in general and particularly for Ni(II) removal. The electrokinetic studies have shown that activated carbons with a predominance of basic functional groups have a positive functional group as opposed to a negative surface potential for activated carbons with a predominance of acidic functional groups [59]. However, the surface charge of activated carbon can be modified by the pH of the external solutions. This parameter must therefore be an important variable that affects the adsorption process, especially of metal ions [60]. Most metals become less soluble and form hydroxides and oxides as the pH of the solution increases [61]. Therefore, a control of the pH of the solution to the favorable adsorption region of the metal ion is very important. Ni(II) can potentially exist in several species depending on the pH values of Ni(II), Ni $(OH)^+$, $Ni(OH)_2^0$, $Ni(OH)_3^-$ and $Ni(OH)_4^{2-}$. Ni(II) appears mainly in cationic form (Ni^{2+}) at pH 7, and its removal was related to adsorption performance. The study of nickel adsorption on OS-AC, C-AC, MOS-AC and MC-AC is carried out, depending on the case, for pH values between 3 and 7 (to avoid nickel precipitation), basic pH values were not considered. This pH range was chosen to examine the evolution of the adsorption of this pollutant associated with the different chemical forms present as a function of pH. The latter is adjusted if necessary, with concentrated sodium hydroxide and hydrochloric acid. The results of Ni(II) adsorption as a function of pH are shown in Figs.11 and 12.

The percentage of Ni(II) metal ions removal as a function of solution pH for modified and unmodified activated carbons is shown graphically below. We can conclude that adsorption is highly pH dependent. The increase in the pH of the solution allows a better extraction of metal ions. The best adsorption rate is observed at a pH of 5.5 for C-AC and 6.0 for MC-AC. The one on OS-AC and MOS-AC is better at a pH value of 6.5. This indicates that OS-AC is not very different from MOS-AC for the removal of Ni(II) at low pH. Maximum adsorption capacity at pH of 6.5 has been reported for commercial carbon-based powdered activated carbon (PAC) modified with nitric acid [62].

The gradual decrease in Ni(II) uptake at low pH is generally due to the competition of H^+ ions with those of Ni(II) for adsorption. The decrease in adsorption at pH>7 is probably due to the precipitation of the metal as nickel hydroxide and the formation of a negative charge on the surface of the activated carbon, resulting in a reduction in their binding. In order to achieve high efficiency and selectivity, the value of 6.5 was chosen as the pH for the metal cation. According to surface complex formation theory (SCF), the increase in the amount of adsorbed metal ions can be explained by a decrease in the competition between protons and metal ions for surface sites, and by the decrease in the positive surface charge [63]. This is also due to the fact that at low pH, there is an electrostatic repulsion between the metal ions and the surface of the positively charged coal. When the pH increases, the metal ion can replace the hydrogen ion on the surface of the adsorbent, resulting in better adsorption [59, 64]. In addition, the surface of the activated carbons studied has a net positive or negative charge that depends on the pH of the solution and the pHpzc. The pHpzc values of the OS-AC and MOS-AC were 6.22 and 3.63 respectively. At a pH lower than these points, protons compete with Ni(II) cations. The maximum adsorption of Ni(II) on OS-AC and MOS-AC was observed for a pH of 6.5 (pH>pHpzc), the same remark was observed with MC-AC (pH=6.5) compared to pHpzc = 6.07 (pH>pHpzc), the charge on the surface of the activated carbon changes to negative, resulting in a greater electrostatic attraction of the nickel cations, resulting in better nickel fixation. As the pH becomes more and more basic, there is competition between the OH^- ions in the solution and the negative charge of the activated carbon, which reduces nickel fixation. For C-AC, nickel adsorption is better with pH of 5.5 compared to pHpzc around 6.44 (pH<pHpzc). This variation is also explained by the nature of the surface area of the activated carbon used. The characteristics of these adsorbents used in terms of specific surface area, micro and mesoporosity, and functional groups on the surface.

The acidic functional groups on the surface of activated carbons serve as ion-exchange sites for metals. To allow cationic adsorption, the pH of the solution must be close to the pKa values of the functional groups. The pH behaviour of nickel ion adsorption suggests that there are weakly acidic groups in the adsorbents that are responsible for ion fixation. The carboxyl group may well be this agent because it begins to dissociate at pH 4–6 in the weakly acidic ionic exchange.

III.10. Nickel Adsorption isotherms

In order to optimize the design of the adsorption process, it is important to establish the best appropriate correlation for the equilibrium curves. Two well known isotherm-models were used, namely Langmuir and Freundlich models. The Freundlich model is well adapted to describe the aqueous phase equilibrium [65]. The model given by equation (5) generally describes adsorption tests taking place on heterogeneous adsorbents and

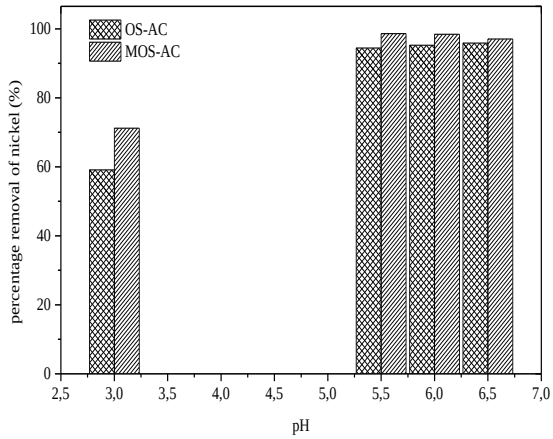

Fig 11. *Effect of initial pH solutionson the percentage removal of Ni(II) onto the OS-AC and MOS-AC (C_0= 100 mg.L^{-1})*

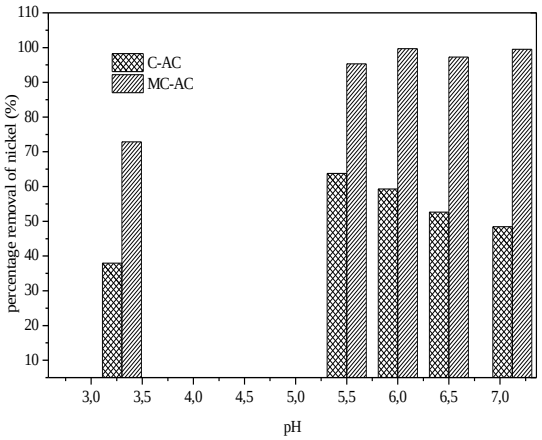

Fig 12. *Effect of initial pH solutionson the percentage removal of Ni(II) onto the C-AC and MC-AC (C_0= 100 mg.L^{-1})*

defines the exponential distribution of active sites and their energies.

$$q_e = K_F \cdot C_e^{\frac{1}{n}} \quad (5)$$

K_F is a constant that indicates the relative adsorption capacity of the adsorbent (mg.g^{-1}) and 1/n indicates the adsorption intensity.

$$q_e = \frac{K_L \cdot b \cdot C_e}{1 + K_L \cdot C_e} \quad (6)$$

q_e: the equilibrium adsorption capacity (mg. g^{-1});
C_e: the equilibrium concentration (mg. L^{-1});
b: the maximum single-layer adsorption capacity (mg. g^{-1});
K_L: the Langmuir binding constant (L.mg^{-1}).
And the Langmuir model expressed by equation (6), derived from kinetics, generally assumes that the adsorption process takes place at specific homogeneous sites within the adsorbent [66].
Figs.13 and 14 show Ni(II) equilibrium uptake the studied adsorbents. These uptake increases with concentration until saturation is attained. A non-linear regression was used to determine parameters for this isotherm to ensure more accurate results [67]. To find the model equation describing the experimental data of Ni(II) adsorption of all samples, four well-known error functions were used in this worknamely: R^2, χ^2, *RMSE* and *APE*. The greater R^2 and smaller χ^2 and RMSE values of Langmuir and Freundlich models are a good indicator for better fitting for considered models.Also, in Figs.13 and 14 are shown the theoretical and experimental adsorption dataaccording to the Langmuir and Freundlich models and their corresponding and related error function values are shown in Table2.

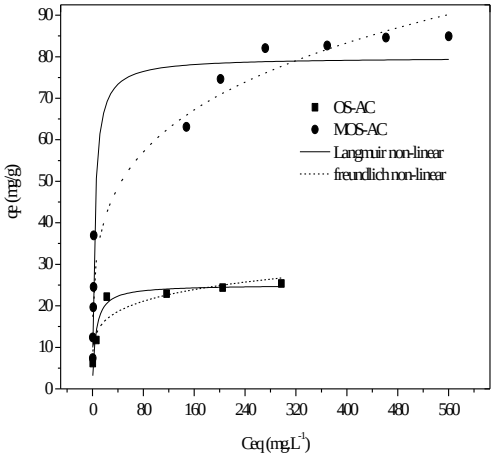

Fig 13. *Non-Linear fitting of the Langmuir and Freundlich isotherms models of Ni(II) for OS-AC and MOS-AC samples*

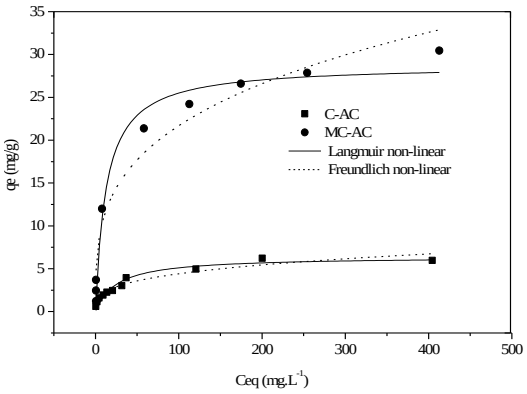

Fig 14. *Non-Linear fitting of the Langmuir and Freundlich isotherms models of Ni(II) for C-AC and MC-AC samples*

Figs. 13 and 14 show isotherms models of Langmuir and Freundlich for Ni(II) adsorption onto the different activated carbons, for an optimal pH. The Langmuir model was the most consistent for

Table 2. Non-Linear Langmuir and Freundlich isotherms parameters of Ni(II)

Adsorbent	OS-AC	C-AC	MOS-AC	MC-AC
Initial pH	6.5	5.5	6.5	6.0
Langmuir				
b (mg.g^{-1})	*25.056*	*6.408*	*79.832*	*28.768*
K_L (L.mg^{-1})	*0.204*	*0.039*	*0.282*	*0.077*
R^2	***0.928***	***0.938***	***0.957***	***0.978***
χ^2	*3.280*	*2.767*	*94.167*	*4.913*
RMSE	*2.036*	*0.457*	*10.746*	*1.793*
APE	*13.301*	*21.374*	*27.378*	*20.867*
Freundlich				
K_F	*9.591*	*1.089*	*20.383*	*5.611*
n	*5.558*	*3.292*	*4.255*	*3.406*
R^2	***0.832***	***0.938***	***0.958***	***0.956***
χ^2	*2.819*	*0.613*	*19.070*	*4.676*
RMSE	*3.187*	*0.480*	*6.962*	*2.316*
APE	*15.324*	*15.844*	*23.316*	*46.217*

adsorption of Ni(II) with high R^2 (0.928, 0.938, 0.957 and 0.978), good χ^2 (3.28, 2.767, 94.167 and 4.913) and low RMSE (2.037, 0.457, 10.746 and 1.793) for OS-AC, AC, MOS-AC and MC-AC respectively, followed by Freundlich isotherm, with a high R^2 (0.938, 0.958 and 0.956), a good χ^2 (0.613, 19.07 and 4.676) and a low RMSE (0.480, 6.962 and 2.316) respectively in the case of C-AC, MOS-AC and MC-AC. The Chi-squared (χ^2) and RMSE values were found to be low in Langmuir isotherm which validates its applicability for non-linear model as the best fitted model. The APE (average percentage error) is significant, ranging from 13% to 27%, confirmed by the discrepancy between experimental and calculated results. The performance of adsorbents for the removal of Ni(II) in aqueous solution are attributed from the maximum monolayer adsorption capacity, without any nickel-nickel interactions. The MOS-AC to give better results for nickel adsorption with a maximum adsorption capacity of 79.83 mg.g^{-1} significantly higher than that obtained by OS-AC with b= 25.05 mg.g^{-1}. A value of 34.48 mg of Ni(II)/g of Salsola plant was reported [68]. For OS-AC and MOS-AC carbons, an energy constant K_L related to the adsorption heat of 0.204 and 0.282 L.mg^{-1} was obtained, respectively.

The nitric acid surface modification improves the Ni(II) adsorption capacity by 218.8%. The removal of Ni(II) on the MC-AC is higher than that of C-AC. The MC-AC has a value of b equal to 28.76 mg.g^{-1} which is significantly higher than the C-AC with b= 6.40 mg.g^{-1}, this means that the MC-AC has a better nickel adsorption potential with an improvement rate of 349.37%. The comparative study of the two activated carbons shows that activated carbon from unmodified olive stones has an efficiency of Ni(II) removal equal to the unmodified commercial activated carbon. All the studied activated carbons have a higher affinity towards Ni(II) as evidenced by the H-type class of the non-linear Langmuir isotherms according to the classification by Giles et al. [68]. Class H also shows a complete adsorption in low concentration. The higher affinity of modified activated carbons for Ni(II) implies that oxidation with nitric acid improves the removal capacity of metal ions. This affinity also due to the presence of large quantities of acid functional groups that can exchange their protons with the nickel cations present in aqueous solution.

The Freundlich model describes well the adsorption isotherm of Ni(II) by MOS-AC, C-AC and MC-AC as R^2 values were 0.958, 0.958 and 0.956 respectively. The values of *n* of 4.25, 3.29 and 3.40, respectively, showing some heterogeneity in the adsorbent surface and the favorability of the adsorption processes. These values show a significant affinity between Ni(II) and the three activated carbons. The Freundlich model slightly describes the adsorption of Ni(II) on OS-AC with R2= 0.83 and n in the order of 5.55. Moreover, the K_F constant is 20.38 for MOS-AC and 5.61 for MC-AC. The value of 20.38 for MOS-AC is quite high compared to the other three coals, which shows the adsorption capacity obtained.

III.11. Adsorption kinetic experiments

Several kinetic models are used to examine the controlling mechanism of adsorption process such as chemical reaction, diffusion control and mass

transfer. Among them, the pseudo-first-order expressed by equation (7) [69] is largely used:

$$\frac{dq_t}{dt} = K_1(q_e - q_t) \quad (7)$$

Where qe and q_t are amounts of Nickel adsorbed ($mg.g^{-1}$) at equilibrium and time t (min), respectively, and K_1 is the rate constant of pseudo-first-order (min^{-1}).

The pseudo-second-order kinetic model expressed by equation (8) [70, 71] is also quite used:

$$\frac{dq_t}{dt} = K_2(q_e - q_t)^2 \quad (8)$$

Where K_2 is the rate constant of pseudo-second-order adsorption ($g.mg^{-1}.min^{-1}$) and $h = K_2.q^2_e$, where h is the initial adsorption rate ($mg.g^{-1}.\ min^{-1}$). The rate parameter for intraparticle diffusion is determined using the following equation [71]:

$$q_t = K_{dif}t^{1/2} + C \quad (9)$$

Where C is a constant that gives an idea about the boundary layer thickness ($mg.g^{-1}$) and K_{dif} is the intraparticle diffusion rate constant ($mg.g^{-1}.min^{-1/2}$). The plot may present multilinearity, indicating that three steps take place. The first, sharper portion is attributed to the diffusion of adsorbate through the solution to the external surface of adsorbent or the boundary layer diffusion of solute molecules. The second portion describes the gradual adsorption stage, where intraparticle diffusion is rate limiting and the third portion is attributed to the final equilibrium stage [72].

The kinetic adsorption tests must be carried out by taking contact times shorter than the equilibrium time, with the doses and optimum pH values found for each activated carbon. Non-linear kinetic models are being fitted (Figs. 15~18) and kinetic data estimated in Table 3.

Adsorption kinetic study involves fitting of the experimental data towards validation of model applicability to adsorption process. However production of extensively different kinetic parameter values in linearized forms has been raised as major problem in adsorption process [73]. So, non-linear regression was suggested to avoid this problem for more accuracy andin data description [74]. The pseudo-first order model well described the adsorption data for C-AC at two different concentrations (100 and 200 $mg.L^{-1}$) as evidenced by high determination coefficient R^2 (0.974 and 0.962), low *RMSE* (0.148 and 0.384) and good χ^2 (0.122 and 1.422) values.

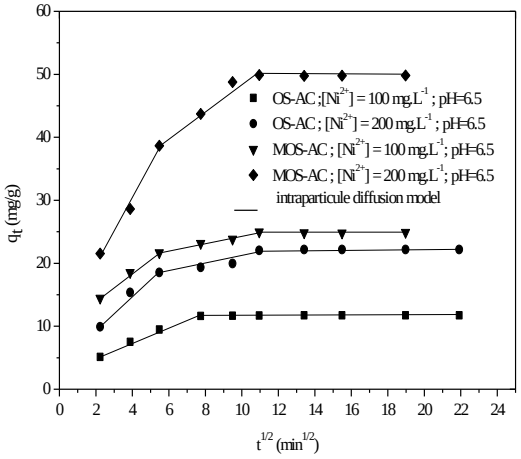

Fig 16. *Different steps of Intra-particle diffusion kinetics model for the adsorption of Ni^{2+}onto OS-AC and MOS-AC for two different concentrations, (T = 25 °C)*

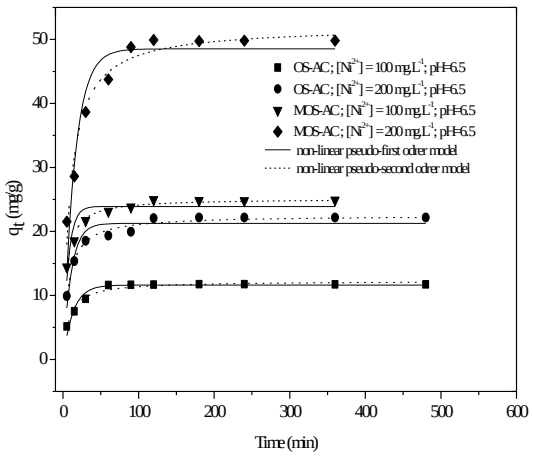

Fig 15. *Non-linear pseudo-first and second order kinetic model for Ni^{2+} onto OS-AC and MOS-AC for two different concentrations, (T = 25 °C)*

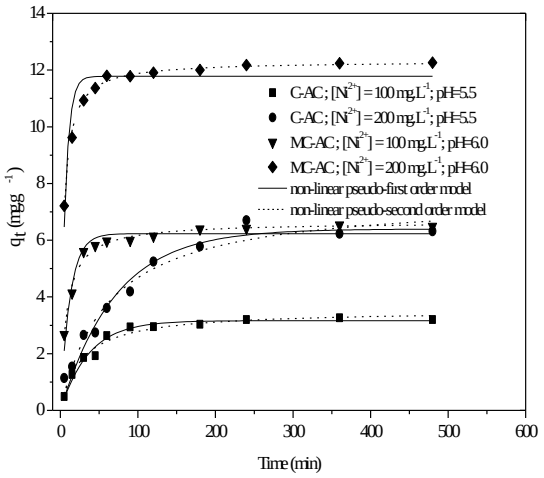

Fig 17. *Non-linear pseudo-first and second order kinetic model for Ni^{2+} onto C-AC and MC-AC for two different concentrations, (T = 25 °C)*

Table 3. Non-linear Kinetic model parameters for the adsorption of Ni(II) onto adsorbents studied at different initial concentrations.

Adsorbent	OS-AC		C-AC		MOS-AC		MC-AC	
Initial pH	6.5		5.5		6.5		6.0	
C_0 *(mg.L^{-1})*	100	200	100	200	100	200	100	200
$q_{e(exp)}$ *(mg.g^{-1})*	11.740	22.184	3.266	3.225	24.977	49.895	3.218	*12.020*
Pseudo-first-order								
K_1 *(min)*	0.076	0.094	0.027	0.014	0.144	0.066	0.082	0.160
$q_{e(cal)}$ *(mg.g^{-1})*	11.616	21.260	3.162	6.397	23.902	48.518	6.231	11.778
R^2	**0.924**	**0.880**	**0.974**	**0.962**	**0.787**	**0.876**	**0.936**	**0.852**
χ^2	0.686	0.884	0.122	1.422	0.985	5.397	0.238	0.317
RMSE	0.643	1.356	0.148	0.384	1.632	3.752	0.302	0.592
APE	5.027	6.675	6.531	11.966	6.205	8.011	5.326	4.236
Pseudo-second-order								
K_2 *(g.mg^{-1}.min^{-1})*	0.130	0.147	0.037	0.016	0.236	0.105	0.132	0.270
$q_{e(cal)}$ *(mg.g^{-1})*	12.251	22.506	3.530	7.518	25.133	52.01	6.638	12.320
h (mg.g^{-1}. min^{-1})	15.911	74.458	0.461	0.904	149.073	284.030	5.816	40.981
R^2	**0.966**	**0.978**	**0.974**	**0.960**	**0.970**	**0.960**	**0.983**	**0.993**
χ^2	0.157	0.310	0.088	0.786	0.128	1.265	0.048	0.015
RMSE	0.430	0.915	0.149	0.396	0.590	2.171	0.165	0.129
APE	3.462	2.832	4.503	9.786	2.050	4.792	2.150	0.850
Intraparticule diffusion								
K_{dif} *(mg.g^{-1}.min$^{-1/2}$)*	0.837	0.500	0.063	0.432	0.580	2.171	0.091	0.163
C	4.572	15.711	2.216	0.163	18.471	26.986	5.172	10.242
R^2	**0.916**	**0.852**	**0.840**	**0.956**	**0.984**	**0.961**	**0.976**	**0.703**
χ^2	0.318	0.051	0.008	0.037	0.003	0.047	0.002	0.012
RMSE	1.056	0.732	0.089	0.253	0.202	1.063	0.063	0.218
APE	9.433	2.031	1.913	3.316	0.550	1.238	0.721	1.142

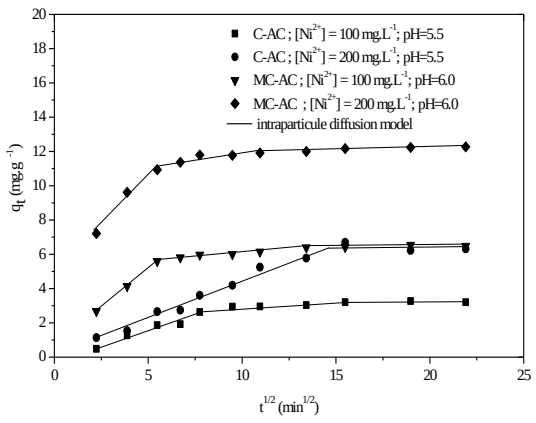

Fig 18. *Different steps of Intra-particle diffusion kinetics model for the adsorption of Ni^{2+} on C-AC and MC-AC for two different concentrations, (T = 25 °C)*

In addition, the predicted equilibrium adsorption capacity (q_e) for C-AC is 3.162 mg.g^{-1} at initial concentrationof100 mg.L^{-1}. These results show that the adsorption of Ni(II), onto C-AC follows the pseudo-first kinetic model. Thus, it can be concluded that the adsorption rate of Ni(II) ions on C-AC depends on the properties of the adsorbate and adsorbent [75]. The pseudo-first-order is not representative for Nickel adsorption onto OS-AC, MOS-AC and MC-AC. This model assumes that the limiting step, the adsorption is the chemisorption that involves electron exchanges at the solid-liquid interface [76,77]. The intraparticular diffusion equation was also applied to the experimental results by plotting q_t versus $t^{1/2}$ for two different Ni(II) concentrations. From the results shown in Table 3, we observed that there are three linear steps. At the beginning of the adsorption there is a linear region which represents

the rapid recovery of the surface, follows a second linear step which represents the diffusion in the pores, and finally a horizontal linear region which represents the adsorption equilibrium. The parameters K_{dif} and C are determined from the second linear step. The parameter C is proportional to the thickness of the boundary layer, which gives an indication of the diffusion of Ni(II) ions towards the adsorbent. This model slightly describes the kinetics of adsorption of Ni(II) by C-AC for the concentration 100 $mg.L^{-1}$ followed by MC-AC for the concentration 200 mg. L^{-1}. For C-AC, the values of C indicate that intraparticle diffusion may not be the controlling factor in determining the kinetics of the process and film diffusion controls the initial rate of the adsorption. The diffusion rate constant (K_{dif}), increases with initial concentration increase. The K_{dif} values are respectively 2.171 and 0.837 $mg.g^{-1}.min^{-1/2}$ for MOS-AC and OS-AC, which means that the diffusion of Ni(II) in the pores is rapid, also we can note that C varies from 4.572 to 26.986 $mg.g^{-1}$, corresponding to the thickness of the boundary-layer increase. The curves indicate a linear characteristic in which intraparticle diffusion drives the adsorption process.

IV. Conclusion

Activated carbon is known for its effectiveness in removing pollutants such as heavy metals from water and wastewater. Nitric acid (4 N) is used to modify the activated carbon surface locally prepared in the laboratory in order to improve its adsorptive capacity toward Ni(II) ions. Tests results show that for Ni(II), the modified activated carbon from olive stones gives better results compared to olive stones-based activated carbon. For commercial activated carbon, oxidation is more effective compared to the unmodified activated carbon. To gain more insight, further characterization is carried out on all adsorbents studied (B.E.T, DRX, XPS, FTIR, iodine number and pH_{pzc}). XRD study reveals the high percent of carbon and the existence of an amorphous phase in the materials investigated. XPS analysis shows that the nitric acid treatment considerably modifies the surface of the activated carbons studied by increasing the quantity of oxygenated functional groups, which could provide further improvement of the adsorption capacity by creating sites of a chemical nature. Almost similar FTIR spectra, with only slight difference in intensities indicate small differences in surface functional groups. Analysis reveals the presence of acidic groups (phenolic, lactonic, carboxylic and carbonyl), confirmed by pH_{pzc} values. A decrease in equilibrium time for nickel adsorption from 180 min for OS-AC to 120 min for MOS-AC is observed. pH has an important influence on the adsorption process. The nickel adsorption process obeys a pseudo-second-order kinetics, with determination coefficients (R^2) ranging from 0.96 to 0.99. The rate constants for Ni(II) adsorption by modified activated carbons are higher than for unmodified counterparts, accounting for the faster adsorption process for modified carbons. The adsorption isotherms obey the Langmuir and Freundlich models with determination coefficients close to unity. An improvement rate of 235.9% is observed for the nickel adsorption capacities, which are 85.47 $mg.g^{-1}$ for MOS-AC and 25.44 $mg.g^{-1}$ for OS-AC. The commercial activated carbon capacity is 30.58 $mg.g^{-1}$ for MC-AC and 6.30 $mg.g^{-1}$ for C-AC with a 385.31% improvement rate. The increase in adsorption rates on the oxidized activated carbon is mainly due to the presence of acidic groups on the surface. This study shows that both activated carbons could be modified chemically for successful efficiency improvement.

V. References

1. Stoeckli, H. F. *Porosity in Carbons: Characterization and Applications*; Patrick, J. W., Ed.; Edward Arnold: London, (1995).
2. Ranganathan, K. Adsorption of Hg(II) Ions from Aqueous Chloride Solutions Using Powdered Activated Carbons. *Carbon 41* (5) (2003) 1087-1092.
3. Gupta, V. K.; Suhas, N. A., Agarwal, S., Chaudhary, M., & Tyagi, I.. Removal of Ni (II) Ions from Water Using Scrap Tire. *J. Mol. Liq190* (2014) 215–222.
4. Cole, C. A. *Hazardous and Industrial Waste Proceedings: 21st Mid-Atlantic Conference*, 1 edition.; Long, D. A., Ed.; CRC Press: Lancaster, Pa., (1989).
5. Bowen, H. J. M. *Environmental Chemistry of the Elements*.; Academic Press., (1979).
6. Dean, J. G.; Bosqui, F. L.; Lanouette, K. H. Removing Heavy Metals from Waste Water. *Environ. Sci. Technol 6* (1972) 518-522.
7. Brinckman, F. E.; Olson, G. J. Chemical Principles Underlying Bioleaching of Metals from Ores and Solid Wastes, and Bioaccumulation of Metals from Solutions. In *Biotechnology and bioengineering symposium* (1986) 35-44.
8. Cerjan-Stefanović, Š.; Kaštelan-Macan, M. Ion Exchange Separation Ag(I) from Waste Waters. *Int. J. Environ. Anal. Chem 38* (1990) 323-328.
9. Tiwari, D. P.; Promod, K.; Mishra, A. K.; Singh, R. P.; SRIVASTAV, R. S. Removal of Toxic Metals from Electroplating Industries (Effect of PH on Removal by Adsorption). *Indian J. Environ. Health 31* (1989) 120-124.
10. Shukla, N.; Pandey, G. S. Charred Waste of Oxalic Acid Plant as an Adsorbent of Toxic Ions and Dyes. *Biol. Wastes 32* (1990) 145-148.
11. Nassar, M. M. The Kinetics of Basic Dye Removal Using Palm-Fruit Bunch. *Adsorpt. Sci. Technol. 15* (1997) 609-617.
12. Nassar, M. M. Energy Consumption and Mass Transfer during Adsorption Using Gas and Mechanical Stirring Systems. *Water Res. 32* (1998) 3071-3079.
13. Nassar, M. M. Intraparticle Diffusion of Basic Red and Basic Yellow Dyes on Palm Fruit Bunch. *Water Sci. Technol. 40* (1999) 133.
14. Ho, Y. S.; McKay, G. The Kinetics of Sorption of Divalent Metal Ions onto Sphagnum Moss Peat. *Water Res., 34* (2000) 735-742.
15. Yu, Q.; Matheickal, J. T.; Yin, P.; Kaewsarn, P. Heavy Metal Uptake Capacities of Common Marine

Macro Algal Biomass. *Water Res.*, *33* (1999) 1534-1537.
16. Nassar, M. M.; Magdy, Y. H. Removal of Different Basic Dyes from Aqueous Solutions by Adsorption on Palm-Fruit Bunch Particles. *Chem. Eng. J.*, *66* (1997) 223-226.
17. Scott, J. A.; Palmer, S. J.; Sage, G. K. Metal Adsorption by Bacterial Capsular Polysaccharide Coatings. In *Recent Developments in Ion Exchange*; Springer (1987) 332-338.
18. Yong, P.; Macaskie, L. E. Effect of Substrate Concentration and Nitrate Inhibition on Product Release and Heavy Metal Removal by a Citrobacter Sp. *Biotechnol. Bioeng.*, *55* (1997) 821-830.
19. Malamis, S.; Katsou, E. A Review on Zinc and Nickel Adsorption on Natural and Modified Zeolite, Bentonite and Vermiculite: Examination of Process Parameters, Kinetics and Isotherms. *J. Hazard. Mater.*, *252* (2013) 428-461.
20. Gao, Y.; Yue, Q.; Gao, B.; Sun, Y.; Wang, W.; Li, Q.; Wang, Y. Preparation of High Surface Area-Activated Carbon from Lignin of Papermaking Black Liquor by KOH Activation for Ni(II) Adsorption. *Chem. Eng. J.*, *217* (2013) 345-353.
21. Rivera-Utrilla, J.; Sánchez-Polo, M.; Gómez-Serrano, V.; Alvarez, P. M.; Alvim-Ferraz, M. C. M.; Dias, J. M. Activated Carbon Modifications to Enhance Its Water Treatment Applications. An Overview. *J. Hazard. Mater.*, *187* (2011) 1-23.
22. El-Hendawy, A.-N. A. Influence of HNO3 Oxidation on the Structure and Adsorptive Properties of Corncob-Based Activated Carbon. *Carbon 41* (2003) 713-722.
23. Macias-Garcia, A.; Diaz-Diez, M. A.; Cuerda-Correa, E. M.; Olivares-Marin, M.; Ganan-Gomez, J. Study of the Pore Size Distribution and Fractal Dimension of HNO_3-Treated Activated Carbons. *Appl. Surf. Sci.*, *252* (2006) 5972-5975.
24. Rambabu, N.; Azargohar, R.; Dalai, A. K.; Adjaye, J. Evaluation and Comparison of Enrichment Efficiency of Physical/Chemical Activations and Functionalized Activated Carbons Derived from Fluid Petroleum Coke for Environmental Applications. *Fuel Process. Technol.*, *106* (2013) 501-510.
25. Termoul, M.; Bestani, B.; Benderdouche, N.; Belhakem, M.; Naffrechoux, E. Removal of Phenol and 4-Chlorophenol from Aqueous Solutions by Olive Stone-Based Activated Carbon. *Adsorpt. Sci. Technol.*, *24* (2006) 375-388.
26. Chemrak, M. A.; Benderdouche, N.; Bestani, B.; Benallou, M. B.; Cagnon, B. Removal of Mercury from Natural Gas by a New Activated Adsorbent from Olive Stones. *Can. J. Chem. Eng.*, *96* (2018) 241-249.
27. Önal, Y.; Akmil-Başar, C.; Sarıcı-Özdemir, Ç.; Erdoğan, S. Textural Development of Sugar Beet Bagasse Activated with $ZnCl_2$. *J. Hazard. Mater.*, *142* (2007) 138-143.
28. Kosmulski, M. The pH-Dependent Surface Charging and the Points of Zero Charge. *J. Colloid Interface Sci.*, *253* (2002) 77-87.
29. Kosmulski, M. PH-Dependent Surface Charging and Points of Zero Charge. IV. Update and New Approach. *J. Colloid Interface Sci.*, *337* (2009) 439-448.
30. Salima, A.; Benaouda, B.; Noureddine, B.; Duclaux, L. Application of Ulva Lactuca and Systoceira Stricta Algae-Based Activated Carbons to Hazardous Cationic Dyes Removal from Industrial Effluents. *Water Res.*, *47* (2013) 3375-3388.
31. Kentner, E.; Armitage, D. B.; Zeitlin, H. A Rapid Dimethylglyoxime Method for the Determination of Nickel(II) in Sea Water. *Anal. Chim. Acta*, *45* (1969) 343-346.
32. Pally, D.; Bertagna, V.; Cagnon, B.; Alaaeddine, M.; Benoit, R.; Podvorica, F. I.; Vautrin-Ul, C. Phenylamide-Oxime and Phenylamide Nanolayer Covalently Grafted Carbon via Electroreduction of the Corresponding Diazonium Salts for Detection of Nickel Ions. *J. Electroanal. Chem.*, *817* (2018) 101–110.
33. Benallou, M. B.; Douara, N.; Chemrak, M. A.; Mekibes, Z.; Benderdouche, N.; Bestani, B. Elimination of Malachite Green on Granular Activated Carbon Prepared from Olive Stones in Discontinuous and Continuous Modes. *Algerian J. Environ. Sci. Technol.7* (2021) 1698-1706.
34. Benderdouche, N.; Bestani, B.; Hamzaoui, M. The Use of Linear and Nonlinear Methods for Adsorption Isotherm Optimization of Basic Green 4-Dye onto Sawdust-Based Activated Carbon. (2018).
35. Khelifi, A.; Almazán-Almazán, M. C.; Pérez-Mendoza, M.; Domingo-García, M.; López-Domingo, F. J.; Temdrara, L.; López-Garzón, F. J.; Addoun, A. Influence of Nitric Acid Concentration on the Characteristics of Active Carbons Obtained from a Mineral Coal. *Fuel Process. Technol.*, *91* (2010) 1338-1344.
36. Huang, G.; Shi, J. X.; Langrish, T. A. G. Removal of Cr(VI) from Aqueous Solution Using Activated Carbon Modified with Nitric Acid. *Chem. Eng. J.*, *152* (2009) 434-439.
37. Saka, C. BET, TG–DTG, FT-IR, SEM, Iodine Number Analysis and Preparation of Activated Carbon from Acorn Shell by Chemical Activation with $ZnCl_2$. *J. Anal. Appl. Pyrolysis*, *95* (2012) 21-24.
38. Bestani, B.; Benderdouche, N.; Benstaali, B.; Belhakem, M.; Addou, A. Methylene Blue and Iodine Adsorption onto an Activated Desert Plant. *Bioresour. Technol.*, *99* (2008) 8441-8444.
39. Lu, A.-H.; Zheng, J.-T. Study of Microstructure of High-Surface-Area Polyacrylonitrile Activated Carbon Fibers. *J. Colloid Interface Sci.*, *236* (2001) 369-374.
40. Xiao, Y.; Long, C.; Zheng, M.-T.; Dong, H.-W.; Lei, B.-F.; Zhang, H.-R.; Liu, Y.-L. High-Capacity Porous Carbons Prepared by KOH Activation of Activated Carbon for Supercapacitors. *Chin. Chem. Lett.*, *25* (2014) 865-868.
41. Mohan, D.; Sarswat, A.; Singh, V. K.; Alexandre-Franco, M.; Pittman, C. U. Development of Magnetic Activated Carbon from Almond Shells for Trinitrophenol Removal from Water. *Chem. Eng. J.*, *172* (2011) 1111-1125.
42. Thakur, S.; Pandey, S.; Arotiba, O. A. Development of a Sodium Alginate-Based Organic/Inorganic Superabsorbent Composite Hydrogel for Adsorption of Methylene Blue. *Carbohydr. Polym.*, *153* (2016) 34-46.
43. Aher, A.; Cai, Y.; Majumder, M.; Bhattacharyya, D. Synthesis of Graphene Oxide Membranes and Their Behavior in Water and Isopropanol. *Carbon*, *116* (2017) 145-153.
44. Hazourli, S.; Ziati, M.; Hazourli, A.; Cherifi, M. Valorisation d'un Résidu Naturel Ligno-Cellulosique En Charbon Actif-Exemple Des Noyaux de Dattes. *Rev. Énerg. Renouvelables ICRESD*, *7* (2007) 187-192.
45. Yang, W.; Liu, Y.; Wang, Q.; Pan, J. Removal of Elemental Mercury from Flue Gas Using Wheat Straw Chars Modified by Mn-Ce Mixed Oxides with Ultrasonic-Assisted Impregnation. *Chem. Eng. J.*, *326* (2017) 169-181.

46. Guedidi, H.; Reinert, L.; Soneda, Y.; Bellakhal, N.; Duclaux, L. Adsorption of Ibuprofen from Aqueous Solution on Chemically Surface-Modified Activated Carbon Cloths. *Arab. J. Chem.*, *10* (2017) S3584-S3594.
47. Liu, H.; Gao, Q.; Dai, P.; Zhang, J.; Zhang, C.; Bao, N. Preparation and Characterization of Activated Carbon from Lotus Stalk with Guanidine Phosphate Activation: Sorption of Cd(II). *J. Anal. Appl. Pyrolysis*, *102* (2013) 7-15.
48. de Celis, J.; Amadeo, N. E.; Cukierman, A. L. In Situ Modification of Activated Carbons Developed from a Native Invasive Wood on Removal of Trace Toxic Metals from Wastewater. *J. Hazard. Mater.*, *161* (2009) 217-223.
49. Bedane, A. H.; Guo, T.; Eić, M.; Xiao, H. Adsorption of Volatile Organic Compounds on Peanut Shell Activated Carbon. *Can. J. Chem. Eng.*, *97* (2019) 238-246.
50. Chen, L.-C.; Peng, P.-Y.; Lin, L.-F.; Yang, T. C. K.; Huang, C.-M. Facile Preparation of Nitrogen-Doped Activated Carbon for Carbon Dioxide Adsorption. *Aerosol Air Qual. Res.*, *14* (2014) 916-927.
51. Ouldmoumna, A.; Reinert, L.; Benderdouche, N.; Bestani, B.; Duclaux, L. Characterization and Application of Three Novel Biosorbents "Eucalyptus Globulus, Cynara Cardunculus, and Prunus Cerasefera" to Dye Removal. *Desalination Water Treat.*, *51* (2013) 3527-3538.
52. Socrates, G. *Infrared and Raman Characteristic Group Frequencies : Tables and Charts* ; John Wiley & Sons (2004).
53. Li, Z.; Ma, Z.; van der Kuijp, T. J.; Yuan, Z.; Huang, L. A Review of Soil Heavy Metal Pollution from Mines in China: Pollution and Health Risk Assessment. *Sci. Total Environ.*, *468-469* (2014) 843-853.
54. Sambaza, S. S.; Masheane, M. L.; Malinga, S. P.; Nxumalo, E. N.; Mhlanga, S. D. Polyethyleneimine-Carbon Nanotube Polymeric Nanocomposite Adsorbents for the Removal of Cr^{6+} from Water. *Phys. Chem. Earth Parts ABC*, *100* (2017) 236-246.
55. Yao, S.; Zhang, J.; Shen, D.; Xiao, R.; Gu, S.; Zhao, M.; Liang, J. Removal of Pb(II) from Water by the Activated Carbon Modified by Nitric Acid under Microwave Heating. *J. Colloid Interface Sci.*, *463* (2016) 118-127.
56. Rao, G. P.; Lu, C.; Su, F. Sorption of Divalent Metal Ions from Aqueous Solution by Carbon Nanotubes: A Review. *Sep. Purif. Technol.*, *58* (2007) 224-231.
57. Abd El-Magied, M. O.; Elshehy, E. A.; Manaa, E.-S. A.; Tolba, A. A.; Atia, A. A. Kinetics and Thermodynamics Studies on the Recovery of Thorium Ions Using Amino Resins with Magnetic Properties. *Ind. Eng. Chem. Res.*, *55* (2016) 11338-11345.
58. Edwin Vasu, A. Surface Modification of Activated Carbon for Enhancement of Nickel(II) Adsorption. *E-J. Chem.* 5, *5*, e610503.
59. Rivera-Utrilla, J.; Ferro-Garcia, M. A. Study of Cobalt Adsorption from Aqueous Solution on Activated Carbons from Almond Shells. *Carbon*, *25* (1987) 645-652.
60. Teker, M.; Saltabaş, Ö.; İmamoğlu, M. Adsorption of Cobalt by Activated Carbon from the Rice Hulls. *J. Environ. Sci. Health Part Environ. Sci. Eng. Toxicol.*, *32* (1997) 2077-2086.
61. Bjerrum, N. Studien Über Chromichlorid. III: Hydroxoaquochromichloride. *Z. Für Phys. Chem.*, *73U* (1910) 724-759.
62. Su, P.; Zhang, J.; Tang, J.; Zhang, C. Preparation of Nitric Acid Modified Powder Activated Carbon to Remove Trace Amount of Ni(II) in Aqueous Solution. *Water Sci. Technol.*, *80* (2019) 86-97.
63. Seco, A.; Marzal, P.; Gabaldón, C.; Ferrer, J. Study of the Adsorption of Cd and Zn onto an Activated Carbon: Influence of pH, Cation Concentration, and Adsorbent Concentration. *Sep. Sci. Technol.*, *34* (1999) 1577-1593.
64. Cho, E. H.; Pitt, C. H. The Adsoption of Gold and Silver Cyanide from Solution by Activated Charcoal, Gold, Silver, Uranium, and Coal Geology, Mining, Extraction and the Environment, The American Institute of Mining, Metallurigal and Petroleum Engineers. *Inc N. Y. NY*, (1983) 114-133.
65. Freundlich, H. M. F. Over the Adsorption in Solution. *J Phys Chem*, *57* (1906) 1100-1107.
66. Langmuir, I. The constitution and fundamental properties of solids and liquids. Part i. solids. *J. Am. Chem. Soc.*, *38* (1916) 2221-2295.
67. Hamid Reza Ghaffari; Hasan Pasalari; Abdolhamid Tajvar; KavoosDindarloo; Ba; bak Goudarzi; Vali Alipour; Amin Ghanbarneajd. Linear and Nonlinear Two-Parameter Adsorption Isotherm Modeling : A Case-Study, (2017).
68. Benderdouche, N.; Bestani, B.; Benstaali, B.; Derriche, Z. Enhancement of the Adsorptive Properties of a Desert Salsola Vermiculata Species. *Adsorpt. Sci. Technol.*, *21* (2003) 739-750.
69. Barrett, E. P.; Joyner, L. G.; Halenda, P. P. The Determination of Pore Volume and Area Distributions in Porous Substances. I. Computations from Nitrogen Isotherms. *J. Am. Chem. Soc.*, *73* (1951) 373-380.
70. Ho, Y. S.; McKay, G. Sorption of Dye from Aqueous Solution by Peat. *Chem. Eng. J.*, *70* (1998) 115-124.
71. Ho, Y. S.; McKay, G. Pseudo-Second Order Model for Sorption Processes. *Process Biochem.*, *34* (1999) 451-465.
72. Weber, W. J.; Morris, J. C. Kinetics of Adsorption on Carbon from Solution. *J. Sanit. Eng. Div.*, *89* (1963) 31-60.
73. Vázquez, G.; Mosquera, O.; Freire, M. S.; Antorrena, G.; González-Álvarez, J. Alkaline Pre-Treatment of Waste Chestnut Shell from a Food Industry to Enhance Cadmium, Copper, Lead and Zinc Ions Removal. *Chem. Eng. J.*, *184* (2012) 147-155.
74. Vithanage, M.; Mayakaduwa, S. S.; Herath, I.; Ok, Y. S.; Mohan, D. Kinetics, Thermodynamics and Mechanistic Studies of Carbofuran Removal Using Biochars from Tea Waste and Rice Husks. *Chemosphere*, *150* (2016) 781-789.
75. El-Magied, A.; O, M. Sorption of Uranium Ions from Their Aqueous Solution by Resins Containing Nanomagnetite Particles. *J. Eng.*, *2016* (2016) e7214348.
76. Mohan, D.; Singh, K. P.; Singh, V. K. Trivalent Chromium Removal from Wastewater Using Low Cost Activated Carbon Derived from Agricultural Waste Material and Activated Carbon Fabric Cloth. *J. Hazard. Mater.*, *135* (2006) 280-295.
77. Carrott, P. J. M.; Carrott, M. R. Lignin–from Natural Adsorbent to Activated Carbon: A Review. *Bioresour. Technol.*, *98* (2007) 2301-2312.

Please cite this Article as:
Termoul M., Bestani B., Benderdouche N., Chemrak M.A., Attouti S., Surface Modification of Olive Stone-based Activated Carbon for Nickel Ion removal from synthetic wastewater***, Algerian J. Env. Sc. Technology, 8*:1 (2022) 2291-2306**